Supplementary Information: Optimal morphokinematics for undulatory swimmers at intermediate Reynolds numbers

Wim M. van Rees[1], **Mattia Gazzola**[2], **and Petros Koumoutsakos**[1] *

[1]Chair of Computational Science, ETH Zurich, Switzerland
[2]School of Engineering and Applied Sciences, Harvard University, USA

1. Optimization history and results

Figure 1 presents the evolution of our optimization process for each of the two cost functions. The corresponding table shows the values of each of the parameters for both our optimal solutions, as well as the initial condition. Figure 3 shows forward and lateral velocities, as well the efficiency, as a function of time for each optimal solution.

2. Effect of swimming frequency

We noted in the main text the high Strouhal number corresponding to both our and Kern & Koumoutsakos (2006) optimal efficient swimmer's, and attributed this to the lower Reynolds number used in these computational works compared with the analyses in Triantafyllou *et al.* (1993); Taylor *et al.* (2003), consistent with Gazzola *et al.* (2014). However, both in Kern & Koumoutsakos (2006) and in the current work, the swimming frequency during the optimization is fixed to $T = 1$. To investigate whether our high Strouhal number is an artefact of fixing T, we simulated our optimal efficient swimmer with swimming periods $T = 0.9$ and $T = 1.1$. The results reported in figure 4 show that the velocity of the swimmers increase only slightly stronger than linearly with their frequencies, so that the Strouhal numbers between these three cases only change by about 2% each. The relative changes in steady-state efficiency are of the same magnitude, so that at least for this regime the efficiency is not sensitive to the swimming frequency. This is consistent with Gazzola *et al.* (2014), where a scaling law was derived based on fluid dynamics arguments that for these simulations would predict $U \propto (T)^{4/3}$, which agrees excellently with our results.

3. Methods

3.1. Numerical method

We consider a self-propelling body immersed in a three dimensional viscous fluid governed by the incompressible Navier-Stokes equations:

$$\nabla \cdot \mathbf{u} = 0, \qquad \frac{\partial \mathbf{u}}{\partial t} + (\mathbf{u} \cdot \nabla)\mathbf{u} = -\frac{1}{\rho}\nabla p + \nu\nabla^2\mathbf{u}, \qquad \mathbf{x} \in \Sigma \setminus \Omega \qquad (3.1)$$

where Σ is the entire domain and Ω is the volume occupied by the swimmer. The no-slip boundary condition at the geometry interface $\partial\Omega$, matches the fluid velocity $\mathbf{u}$ to

* Email address for correspondence: petros@ethz.ch

the local body velocity $\mathbf{u}_s$. The feedback from the fluid to the body follows Newton's equations of motion:

$$m_s\ddot{\mathbf{x}}_s = \mathbf{F}^H, \qquad d(\mathbf{I}_s\boldsymbol{\theta}_s)/dt = \mathbf{M}^H, \qquad (3.2)$$

where $\mathbf{F}^H$ and $\mathbf{M}^H$ are the hydrodynamic force and torque exerted by the fluid on the body, characterised by centre of mass $\mathbf{x}_s$, angular velocity $\boldsymbol{\theta}_s$, mass m_s and moment of inertia $\mathbf{I}_s$.

The numerical method to discretize and advance equations (3.1) and (3.2) in time consists of a remeshed vortex method, with a penalization technique Angot *et al.* (1999) to account for the no-slip boundary condition and a projection method Coquerelle & Cottet (2008); Gazzola *et al.* (2011) to capture the action from the fluid to the body. The body geometry is represented with a characteristic function χ_s ($\chi_s = 1$ inside the body, $\chi_s = 0$ outside and mollified at the interface) and its motion is defined by the deformation velocity field $\mathbf{u}_{\text{def}}$. Further details, validation and verification of the method can be found in Gazzola *et al.* (2011, 2012); van Rees *et al.* (2013). In this study, we discretize the domain with a uniform grid spacing of $h = L/256$ during the optimisation and $h = L/512$ for the diagnostics reported. The mollification length of χ_s is set to $\epsilon = 2\sqrt{2}h$, Lagrangian CFL to $LCFL = 0.1$, and penalization factor $\lambda = 10^4$ Gazzola *et al.* (2011).

3.2. *Cost functions*

In this work we present two optimal morphokinematic solutions, one for maximum speed and one for maximum efficiency, as in van Rees *et al.* (2013). The former is obtained by evaluating the average forward velocity $\overline{U}$ of the swimmer during its sixth swimming cycle:

$$f_{\text{vel}} = -\overline{U} = -\left\|\frac{1}{T}\int_{5T}^{6T}\mathbf{U}(t)\,\mathrm{d}t\right\|_2, \qquad (3.3)$$

where the sign is inverted in case the swimmer moves backwards. The most efficient solution is found by minimizing the Froude efficiency over the sixth swimming cycle:

$$f_{\text{eff}} = -\frac{E_{\text{useful}}}{E_{\text{input}} + E_{\text{useful}}} = -\frac{\rho V_s\overline{U}^2/2}{\left(\frac{1}{T}\int_{5T}^{6T}P_{\text{input}}(t)\,\mathrm{d}t\right) + \rho V_s\overline{U}^2/2}, \qquad (3.4)$$

where $\rho = 1$ is the swimmer's density, V_s is its volume and P_{input} is the total instantaneous power delivered to the fluid, computed as

$$P_{\text{input}} = \frac{\mathrm{d}}{\mathrm{d}t}\int_{\Sigma\setminus\Omega}\rho\frac{u^2}{2}\,\mathrm{d}V + \mu\int_{\Sigma\setminus\Omega}\left(\nabla\mathbf{u} + (\nabla\mathbf{u})^T\right):\nabla\mathbf{u}\,\mathrm{d}V. \qquad (3.5)$$

For further details on the computation of these metrics, we refer to (Gazzola *et al.* 2012; van Rees *et al.* 2013).

For completeness, we put our efficiency definition in the context of some related efficiency metrics. Specifically, we note that in our optimization algorithm, the efficiency associated with each swimmer is used only for ranking candidate solutions, and it is discarded afterwards. The adaptation of the generation of new candidate solutions is therefore only based on the ordering of solutions, rather than the numerical value of the objective function. This means that as long as a different metric respects the same ranking as ours, it would lead to an identical optimization process and thus the same optimal solution.

As a consequence, our metric for efficiency $\eta = E_{\text{useful}}/(E_{\text{input}} + E_{\text{useful}})$ would give

the same optimum as the metric $\eta_1 = E_{\text{useful}}/E_{\text{input}}$, since $\eta_1 = \eta/(1-\eta)$ is a monotonic function of η as long as $0 < \eta < 1$. Similarly, the metric η_1 would give the same optimum as $\eta_2 = (mg\bar{V}T)/E_{\text{input}}$, where $\bar{V}$ is the average speed over the swimming cycle T, since we define $E_{\text{useful}} = m\bar{V}^2/2$. The efficiency metric η_2 is actually similar to the inverse cost of transport metric Tucker (1970), used in biological contexts to compare the energetic costs of locomotion across different species. Even though in our input energy definition we do not consider physiological effects, our efficiency metric still offers an intuitive interpretation and matches existing approaches in literature.

Alternative metrics for efficiency could take into account the muscular or physiological efficiencies corresponding to biological swimmers. It would be interesting to compare such optima with our current results. However, this goes beyond scope and purpose of the current manuscript, and instead will be considered in future investigations.

3.3. *Optimizer*

Optimal morphokinematic solutions (characterised by $\{\beta_i^w\}_{i=1,\ldots,4}$, $\{\beta_j^h\}_{j=1,\ldots,6}$, $\{\beta_k^m\}_{k=1,\ldots,4}$ and τ) are identified by the stochastic optimisation algorithm Covariance Matrix Adaptation Evolutionary Strategy (CMA-ES) in its multi-host, rank-μ and weighted recombination form Hansen *et al.* (2003). CMA-ES has been shown to be robust and efficient in dealing with flow related optimisation problems Kern & Koumoutsakos (2006); Gazzola *et al.* (2012); van Rees *et al.* (2013). Throughout this work we set the population size $p = 60$, which we found to be a good compromise between robustness and computational cost. We initialise our parameters ($\mathbf{m}_0$) to reproduce the geometry of a zebrafish larva at 5 days post fertilisation (Fig. 2) without any midline deformations.

The search space bounds are enforced through a rejection algorithm. We consider invalid, for numerical reasons, cases in which the vertical coordinate of β_1^w, $\beta_{N_w-2}^w$, β_1^h or $\beta_{N_h-2}^h$ is smaller than the grid spacing used in our simulations. Furthermore, we reject cases in which one or both profile curves cross the body midline or intercross themselves throughout the deformation. Invalid configurations are rejected by assigning a high default cost function value.

3.4. *Choice of number of parameters*

We use fifteen parameters to represent the swimmer's morphokinematics, using five for the gait (four control point curvatures and one controlling the wavelength), six for the height profile and four for the width profile. A larger number of parameters, although likely to improve the representation of fine morphological features and kinematic details, comes at a high computational price. In fact, evolutionary strategies suffer from a curse of dimensionality, so that any increase in the number of optimisation parameters has to be traded off against the corresponding computational cost.

For the midline, the five controlling parameters were found to be able to reproduce a satisfactory range of undulatory swimming gaits in Kern & Koumoutsakos (2006) and in Gazzola *et al.* (2012). For the swimmer's morphology, the parameterization and number of parameters are the same as in van Rees *et al.* (2013). This parameterization was found capable of reproducing a wide range of morphological shapes. The use of six parameters for the height profile allows more complexity for such features as caudal fin and/or dorsal fins. We use only four parameters for the width curve since the representation and functionality of lateral fins is not considered in our computational setup and simulation method. Four parameters for the width profile were found to be sufficient for the representation of a variety of streamlined profiles.
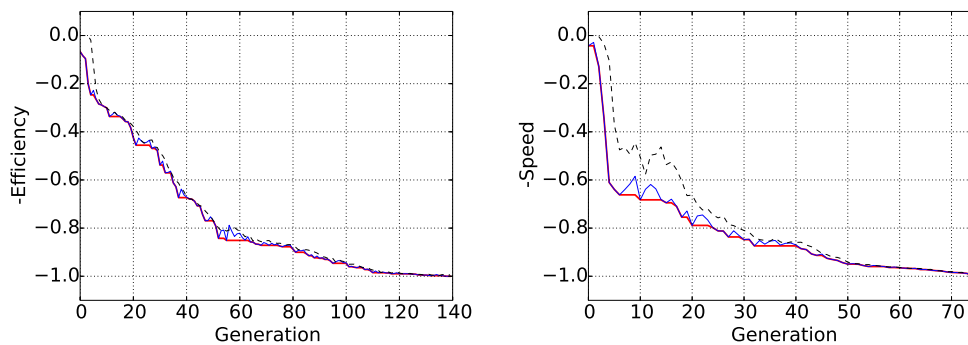
FIGURE 1. The fitness evolution for the efficient (left) and fast (right) swimmer during the optimization. We show the mean per generation (black), the minimum per generation (blue) and the global minimum (green). The y-axes are normalized by their respective optimum values.

REFERENCES

ANGOT, P., BRUNEAU, C.H. & FABRIE, P. 1999 A penalization method to take into account obstacles in incompressible viscous flows. *Numerische Mathematik* **81** (4), 497–520.

COQUERELLE, M. & COTTET, G.-H. 2008 A vortex level set method for the two-way coupling of an incompressible fluid with colliding rigid bodies. *Journal of Computational Physics* **227** (21), 9121–9137.

GAZZOLA, M., ARGENTINA, M. & MAHADEVAN, L. 2014 Scaling macroscopic aquatic locomotion. *Nature Physics* **10**, 758–761.

GAZZOLA, M., CHATELAIN, P., VAN REES, W.M. & KOUMOUTSAKOS, P. 2011 Simulations of single and multiple swimmers with non-divergence free deforming geometries. *Journal of Computational Physics* **230** (19), 7093–7114.

GAZZOLA, M., VAN REES, W. M. & KOUMOUTSAKOS, P. 2012 C-start: Optimal start of larval fish. *Journal of Fluid Mechanics* **698**, 5–18.

HANSEN, N., MULLER, S. D. & KOUMOUTSAKOS, P. 2003 Reducing the time complexity of the derandomized evolution strategy with covariance matrix adaptation (CMA-ES). *Evolutionary Computation* **11** (1), 1–18.

KERN, S. & KOUMOUTSAKOS, P. 2006 Simulations of optimized anguilliform swimming. *Journal of Experimental Biology* **209** (24), 4841–4857.

VAN REES, W.M., GAZZOLA, M. & KOUMOUTSAKOS, P. 2013 Optimal shapes for intermediate Reynolds number anguilliform swimming. *Journal of Fluid Mechanics* **722**.

TAYLOR, G.K., NUDDS, R.L. & THOMAS, A.L.R. 2003 Flying and swimming animals cruise at a strouhal number tuned for high power efficiency. *Nature* **425**, 707–711.

TRIANTAFYLLOU, G.S., TRIANTAFYLLOU, M.S. & GROSENBAUGH, M.A. 1993 Optimal thrust development in oscillating foils with application to fish propulsion. *Journal of Fluids and Structures* **7**, 205–224.

TUCKER, V.A. 1970 Energetic cost of locomotion in animals. *Comparative Biochemistry and Physiology* **34**, 841–846.

	β_1^m	β_2^m	β_3^m	β_4^m	τ			β_1^w	β_2^w	β_3^w	β_4^w
$\mathbf{m}_0$	0	0	0	0	π		$\mathbf{m}_0$	$8.9e^{-2}$	$1.7e^{-2}$	$1.6e^{-2}$	$1.3e^{-2}$
$\mathbf{m}_{\text{eff}}$	-2.9	2.0	-6.1	-2.5	2.4		$\mathbf{m}_{\text{eff}}$	$2.4e^{-1}$	$3.0e^{-1}$	$8.3e^{-3}$	$5.7e^{-3}$
$\mathbf{m}_{\text{fast}}$	2.5	-7.7	-2.2	-2.0	0.76		$\mathbf{m}_{\text{fast}}$	$1.4e^{-1}$	$8.1e^{-2}$	$5.0e^{-3}$	$7.5e^{-3}$

	β_1^h	β_2^h	β_3^h	β_4^h	β_5^h	β_6^h
$\mathbf{m}_0$	$5.5e^{-2}$	$6.8e^{-2}$	$7.6e^{-2}$	$6.4e^{-2}$	$7.2e^{-3}$	$1.1e^{-1}$
$\mathbf{m}_{\text{eff}}$	$2.2e^{-1}$	$2.7e^{-1}$	$2.8e^{-1}$	$3.0e^{-1}$	$3.0e^{-1}$	$2.2e^{-1}$
$\mathbf{m}_{\text{fast}}$	$6.0e^{-2}$	$4.5e^{-2}$	$8.5e^{-2}$	$9.8e^{-2}$	$9.5e^{-2}$	$1.3e^{-1}$

TABLE 1. The optimal solutions' motion (top left), width (top right) and height (bottom) parameters for fast ($\mathbf{m}_{\text{fast}}$) and efficient ($\mathbf{m}_{\text{eff}}$) swimming, as well as for start searching point $\mathbf{m}_0$. The parameters correspond to swimmers with $L = 1$.
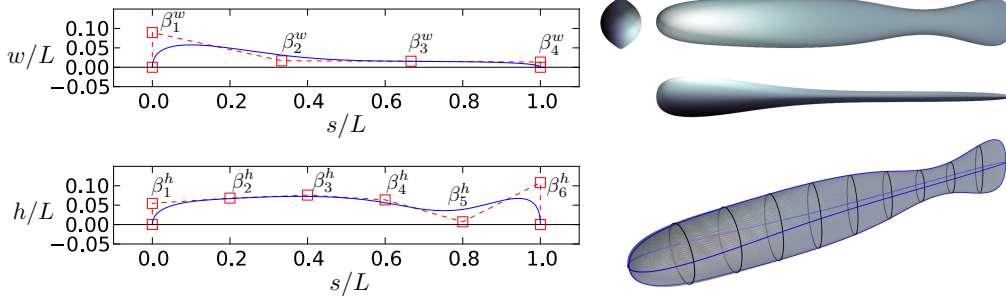

FIGURE 2. Width (top left) and height (bottom left) profile curves, and 3D shape (right) for the larval zebrafish morphology, and starting searching point $\mathbf{m}_0$.
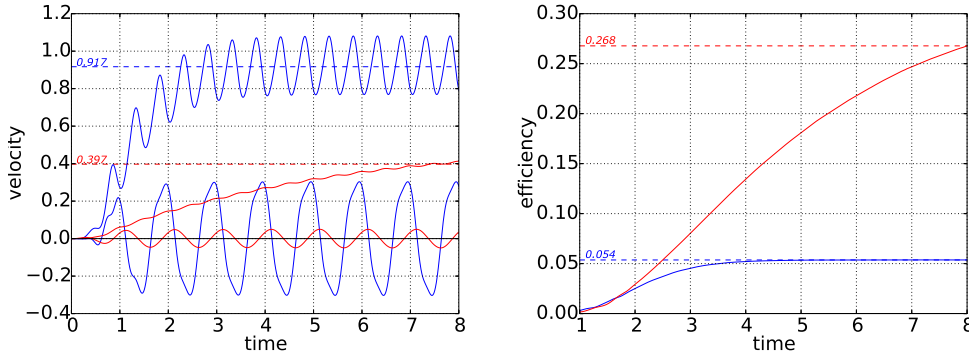

FIGURE 3. The evolution of forward and lateral velocities (left) and efficiency in the last cycle (right) for the fast (blue) and efficient (red) swimmer. The final values are given by the respective numbers above the dashed lines. The numerical data corresponds to swimmers with $L = 1$, $T = 1$ and $Re_{\text{fish}} = 550$.
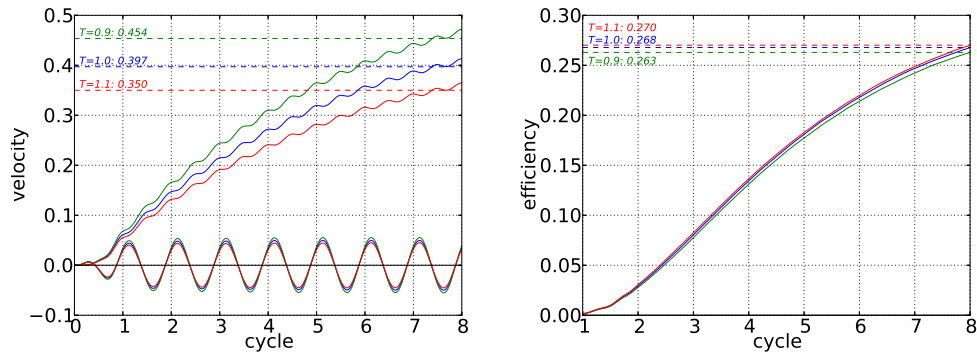
FIGURE 4. Forward and lateral velocities (left) and efficiency over last cycle (right) of the most efficient morphokinematic solution swimming with $T = 0.9$ (green), $T = 1.0$ (blue) and $T = 1.1$ (red). The numerical data corresponds to swimmers with $L = 1$, and $Re_{\text{fish}} = 550$.